# Effect of rotor spinning transfer channel modification on fiber orientation and yarn properties

Huiting Lin[a,c], Nicholus Tayari Akankwasa[a], Josep M Bergadà[b] and Jun Wang*[a]

[a]*Key Laboratory of Textile Science & Technology, Ministry of Education, Donghua University, Shanghai, China;* [b]*Fluid Mechanics Department, UPC-ESEIAAT, Colon 11 E-08222 Terrassa, Spain;* [c]*College of Textile & Apparel, Quanzhou Normal University, Quanzhou, China*

* Corresponding author: E-mail: junwang@dhu.edu.cn.

# Effect of rotor spinning transfer channel modification on fiber orientation and yarn properties

**Abstract**

The vortices are generated at the conventional transfer channel, having adverse effects on fiber configuration. In a former research, a conventional transfer channel was modified via rounding the transfer channel inlet corner and adding a bypass channel. The simulation results obtained with the modified transfer channel showed that the vortices were eliminated and the inlet air velocity increased. We present the impact of this modification on the yarn properties and fiber straightness. Four groups of yarn samples were spun using the conventional and modified spinning system. Yarn properties and fiber straightness along the rotor groove were evaluated. Results revealed that tenacities of the yarns spun on the modified system, increased in comparison to that of the conventionally spun yarns. The number of nearly straight fibers is increased by 25.55% by using the modified system, which was mainly attributed to the decrease in the number of fibers with trailing and leading hooks.

**Keywords:** Rotor spinning, yarn properties, fiber configuration, transfer channel, air flow

## Introduction

Yarn properties differ depending on the yarn spinning methods (Erdumlu et al., (2009); Eldessouki et al., (2015)). Open-end rotor spun yarns are weaker than ring spun yarns of comparable cross section, which is due to the relatively large number of folded fibers and poor distribution of fibers within the yarn structure (Lord, (1971); Pillay et al., (1975)). If fiber orientation is improved during the spinning process, the final rotor spun yarn properties will consequently ameliorate. In rotor spinning, wrapper fibers are formed in the process of twist insertion and yarn formation (Koç & Lawrence, (2006)). The airflow in the rotor spinning channel also influences the fiber configuration significantly, which have been carefully studied (Jin et al., (2016); Lin et al., (2015)). Hooked, looped and entangled fibers may be straightened during the transfer process while new hooked fibers may also be possibly formed (Chattopadhyay, (1988)). The change in fiber configuration occurs during the process of removal from the opening roller pins and transportation to the rotor groove (Murugan et al., (2007); Salhotra et al., (1982)). Straight fibers in the feed sliver may either get hooked or looped during passage through the transfer channel (Chattopadhyay & Sarkar, (1986)). This is mainly generated because of the contact of the fibers with the inner surface of the transfer channel and the impact of transfer channel airflow on the fibers, both effects being related to the transfer channel geometry.

Numerous researchers have studied the effect of the transfer channel geometry on the fiber configuration. (Smith & Roberts, (1994)) reported that a tapered configuration of the transfer channel was useful in straightening fiber crimps and a larger air velocity difference along the channel and a longer duct would result in more oriented fibers. Using high-speed photography, (Lawrence & Chen, (1988)) investigated the manner of fiber detachment from the opening roller pins and the fiber trajectories through the transfer channel. Their investigation showed that a rectangular transfer channel inlet was more beneficial to fiber straightening than a circular one. Based on the observations, they determined a group of empirical equations to optimize the transfer channel design. (Zhang et al., (1991)) indicated that increasing the transfer channel inlet air velocity could help in straightening the leading hook when the fibers were removed from the opening roller. Their analysis also revealed that decreasing the fiber separation area could improve the fiber configuration due to the reduction of air vortex.

(Kong & Platfoot, (1996)) employed a two-dimensional CFD model to simulate the airflow pattern inside the transfer channel. They found that the air flow at the transfer channel inlet was particularly sensitive of the inlet area shape and fiber configuration was greatly influenced by the air flow here. (Kong & Platfoot, (2000), (1997)) further simulated fiber movement inside the transfer channel. They demonstrated that the initial fiber position when entering the transfer channel and the underlying air flow pattern was important in determining the final fiber configuration at the exit of the transfer channel. The occurrence of high recirculation in the transfer channel inlet area would degrade fiber straightness and consequently decrease yarn properties. (Lin et al., (2018)) further developed a three-dimensional CFD model of the rotor spinning unit to study the vortex inside the transfer channel. They reported that the vortices were decreased either increasing the transfer channel length or the rotor outlet relative pressure. Two modifications on the transfer channel inlet shape were proposed to obtain a favorable airflow environment for fiber transportation. The first modification consisted of rounding the connection between the transfer channel and the opening roller cover cap. The idea behind such modification was to avoid a sudden flow shear stresses change in such boundary, thus improving the air flow streamlines. The second one was to add a bypass channel as an external air supply channel to increase the air velocity along the transfer channel. Based on the previous brief literature review, it may be concluded that the air flow inside the transfer channel is greatly affected by the transfer channel geometry, and the airflow performance is a crucial factor in the determination of fiber configuration and yarn properties.

The aim of this research is to study the influence of the modified transfer channel proposed by (Lin et al., (2018)) on fiber straightness and yarn properties. Cotton and viscose yarns with different linear densities were spun using the conventional and modified rotor spinning units and their quality properties were statistically analyzed. To evaluate the fiber straightness in the rotor groove, the tracer fiber technique was employed and the results obtained were compared.

## Materials and methods

### *Rotor spinning unit and 3-D CFD modelling*

Figure 1 depicts the schematic diagram of a conventional rotor spinning unit. When the rotor spinning machine is running, the air inside the rotor will be sucked by a vacuum pump. This leads to the formation of a negative pressure zone in the rotor, forcing the external air to enter the opening roller chamber. Because of the pressure differential generated, an air stream is forced to flow into and along the transfer channel. However, due to the sharp corner existing at the connection between the transfer channel and the opening roller cover cap, a vortex is often generated at the transfer channel inlet, as shown in Figure 1, which reduces the transfer channel inlet flow section and deteriorates the fibers configuration. This scenario was initially reported by (Kong & Platfoot, (1996), (1997), (2000)). Lately, this particular vortex formation was carefully studied by (Lin et al., (2018)). Nevertheless, as the geometry of the transfer channel affects the airflow path, it consequently changes the path of the fibers from the opening roller pins to the rotor groove. For this reason and based on the fact that a rounded corner provides a smoother air flow boundary than a sharp one, the conventional rotor spinning unit was modified, aiming at reducing the vortex to improve fiber configuration.

Figure 2 presents the schematic diagram of the modified rotor spinning unit, which was based on a conventional one. The bypass channel was introduced to increase the air velocity along the transfer channel and it was located on the extension of the long side of the transfer channel. It is to be realized that the behaviour of the airflow when entering the transfer channel will be different thanks to this particular condition. Therefore, the modified rotor spinning unit was developed with the software solid-works and the airflow characteristics were analyzed by using Fluent 6.3.26 CFD software. The simulation was based on the RNG *k*-epsilon turbulence model with real dimensions of the rotor spinning unit used. The boundary conditions were, the rotor air outlet pressure was of -7000 Pa, the rotor speed and the opening roller speed were respectively of 100000 rpm and 6000 rpm. The main dimensions of the rotor spinning unit were as follows: rotor diameter 36 mm, opening roller diameter 65 mm and the transfer channel length 40 mm. The rounded corner radius was 1.5 mm and the bypass inlet area was 5×6 mm. Specific details of the simulation performed, the grid independency test, the Y+ values obtained and a large amount of the simulations performed under different boundary conditions are to be found in (Lin et al., (2018)).

**[Figure 1 here]**

**[Figure 2 here]**

## *Airflow characteristics in the transfer channel*

Figure 3 presents the streamlines of the airflow in the conventional and modified transfer channels. It is observed that the vortex located at the left side of the conventional transfer channel inlet reduces to a very small one in the new design. To compare clearly, the air velocity distributions along the transfer channel inlet (A-A') and the vortex area (B-B') (see Figure 3) are presented in Figure 4. The air velocity along the transfer channel, especially in the fiber separation area is higher in the modified transfer channel compared to the conventional one (see Figure 4(a)). To quantitatively evaluate the air velocity distributions of the conventional and modified transfer channel, the RSD (relative standard deviation) of the velocities along A-A' and B-B', which shows the degree of data dispersion, is calculated and compared respectively. For the velocity along A-A', $RSD_{cA}$ is 117.5%, and $RSD_{mA}$ is 98.8%. For the velocity along B-B', $RSD_{cB}$ is 93.04% while $RSD_{mB}$ is 42.04%. Note that $RSD_{cA}$ and $RSD_{mA}$ are the relative standard deviations of the velocities along A-A' in conventional and modified transfer channel respectively. $RSD_{cB}$ and $RSD_{mB}$ are the relative standard deviations of the velocities along B-B' in conventional and modified transfer channel respectively. The greater the relative standard deviation, the more discrete the data is. Therefore, from the RSD values above, it can be seen that the velocity distribution in the modified transfer channel is more uniform than that in conventional one, which would be more beneficial to the fiber transportation. From Figure 4(b), the *y* velocity (≥ 0 m/s) accounts for less than one quarter (2.5 mm) along B-B' (total 10 mm long). Since the *y* velocity (≥ 0 m/s) means that the air is flowing backward, this indicates that the effective fiber transportation width, defined as the width of a cross section containing forward flow (Kong & Platfoot, 1996), is reduced to about three quarters in the conventional condition.

Fiber transportation along the transfer channel is an air-drafting process. The drawing ratio and fiber straightness improve when the velocity distribution is more uniform and there are no vortices appearing at the transfer channel inlet. The mass flow transported by the transfer channel increases and this is envisaged to be beneficial for the drawing ratio. Fiber straightness is clearly improved when reducing the vortices at the transfer channel inlet. The transfer channel air velocity is mainly determined by the intensity of the negative pressure zone in the rotor. A stronger negative pressure zone in the rotor would lead to a higher transfer channel air velocity. Nevertheless, it is to be noticed that higher energy consumption is required to obtain a higher negative pressure. The bypass channel shown in Figure 2, was therefore used, to increase the air velocity in the transfer channel without the need of increasing the rotor negative pressure, and it is proved to be an effective method according to the simulation results as can be seen in Figure 3.

As the bypass channel is open to the atmosphere, the external air will flow into the bypass channel due to the pressure difference between the rotor and the external environment. For the new configuration, the total mass flow of the air to the rotor consists of two streams. One comes from the bypass channel and the other is from the trash box. In reality, due to the new mass flow coming from the bypass channel, the mass flow from the trash box is smaller than the one existing in conventional units, in any case the overall mass flow is higher in the new developed unit, as proved in (Lin et al., (2018)). This allows higher average air velocity in the fiber transfer channel and decreases air velocity in the trash box. Moreover, the external air from the bypass channel also increases the air velocity in the fiber separation area, which is helpful for fiber removal from the opening roller pins and fiber straightening according to the results reported by (Smith & Roberts (1994); Zhang et al. (1991)).

Both modifications, i.e. rounding the corner and adding the bypass channel, were aiming to improve the fiber straightness and hence yarn tenacity by decreasing the vortex generated at the channel inlet and increasing the air velocity inside the transfer channel.

**[Figure 3 here]**

**[Figure 4 here]**

## *Materials*

Based on the simulations briefly outlined in the present manuscript and carefully addressed in reference (Lin et al. (2018)), a conventional JWF1612-2157A rotor spinning unit was modified. The transfer channel inlet corner, one side of the connection between the transfer channel and the opening roller cover cap, was rounded using a hand file tool. A bypass channel, located on the other side of the transfer channel inlet and having its flow direction tangent to the transfer channel wall was created. The following experiments were then conducted based on the conventional and modified rotor spinning systems.

The characteristics of the raw materials and spinning conditions are shown in Table 1. Two cotton yarns with different linear densities, one viscose yarn and 50:50/cotton: viscose blend yarn were produced using the two spinning systems, respectively. In total, eight yarn samples were produced.

**[Table 1 here]**

## *Methods of testing yarn properties*

Properties of the yarns produced such as tenacity, elongation, hairiness, evenness and imperfections were tested and compared. The yarns were conditioned for at least 24 hours before being tested. Yarn strength was measured on a YG061 yarn strength tester with the constant rate of extension (CRE), at a clamp speed of 500 mm/min and gauge length of 500 mm. Thirty samples were tested in each case. Yarn hairiness was tested on a YG172A yarn hairiness test device at a speed of 30 m/min. Ten samples of 10 m length, a total of 100 m of each yarn were tested. Yarn evenness and imperfections were measured on a Changling CT3000 yarn evenness tester at a speed of 200 m/min. Ten samples of 100 m length, a total of 1000 m of yarn were tested in each case. All the tests were conducted at a temperature of 20 ± 2°C and humidity of 65 ± 2%.

## *Definition of the degree of fiber straightness*

Fiber configuration varies at different stages of rotor spinning, and it has a great impact on yarn properties. Several researchers (Pillay et al., (1975); Lawrence & Jiang, (1996); Lawrence & Chiu, (1996); Lawrence & Chen, (1986)) have studied fiber configuration at different spinning stages and within the yarn structure. They grouped fiber configurations into several categories. In the present study, the classification of fiber configurations proposed by (Lawrence & Chen, (1986)) was used after a small modification. As the U-formed fiber and the folded fiber both had an extent of about half of the fiber length, they were classified in one group. The entangled fiber and transverse entangled fiber were considered as the same class since both of them contributed very little to the yarn strength. Therefore, the modified classification of fiber configuration used in this study for analysis of fiber orientation in the rotor groove is presented in Table 2.

**[Table 2 here]**

In addition to the classification of fiber configuration that provides a qualitative evaluation of fiber straightness, the parameter *S* (Lawrence & Chen, (1988), (1986)) the fiber orientation statistic which is related to fiber shape, is also considered. The parameter *S* is given as:

$$S = (l - l_e)/l \qquad (1)$$

where $l$ is the real fiber length and $l_e$ is the fiber extent, see Figure 5. The statistic S indicates the fiber straightness in the rotor groove. Smaller values of the fiber orientation statistic *S* mean higher fiber straightness.

**[Figure 5 here]**

## *Methods of collecting fiber images*

In order to obtain the fiber images, the tracer fiber technique originally developed by Morton and Summer (Morton & Summers, (1949)) was used in the present investigation. Viscose fibers were used as raw materials. A small quantity of viscose fibers (about 1%) was taken from the sliver and was dyed Mazarine Blue with a direct dyeing. These fibers were then dried in the heat oven at a temperature of 85°C for 5 hours. For purpose of blending the colored fibers within the sliver uniformly, they were put back on the sliver, and the bended sliver was drafted in the drawing frame. The linear density of the final blend sliver thus produced was 1437 tex.

The sliver containing the tracer fibers was fed by the feeding roller to the opening roller. Fibers separated by the opening roller were transported by the air flow through the transfer channel and finally collected in the rotor groove. The machine was stopped after an approximately 6 seconds' fiber feeding. The fiber ring was then carefully removed from the rotor groove with the help of tweezers after the rotor was stopped.

Each fiber ring picked up from the rotor groove was put on the Cano Scan 9000F Mark II and was scanned with a resolution of 1200 dpi in a JPG format. The fiber rings were very thin and each of the collected strands contained one tracer (colored) fiber at most. The fiber images collected showed clearly the shape of the tracer fibers (see Figure 6 (images before processing)). Each tracer fiber was then observed and classified according to the classification described in Table 2. The number of the classified fiber was then recorded. A minimum of 100 tracer fibers for each of the two rotor spinning units were evaluated. Therefore, a whole set of different fiber types as well as the total number of each fiber type for the conventional and modified rotor spinning system was obtained. As for the statistic $S$, the images containing tracer fibers were processed with a code in MATLAB environment and two parameters of $l$ and $l_e$ were calculated. Figure 6 shows two of the original fiber images from the scanner and the schematic diagram of the images after being processed in MATLAB. A total of 100 tracer fibers were evaluated to obtain the average value of parameter $S$ for each rotor spinning unit.

The yarn properties and fiber straightness test results were analyzed by One-way ANOVA at $\alpha$ value of 0.05 for any difference between the means using Minitab 17.0.

**[Figure 6 here]**

## Results and discussion

### *Yarn properties*

*Analysis of tenacity and elongation for different samples*

The average values of yarn tensile properties of the four sets of yarns are presented in Figures 7 and 8. Tenacities of 34 tex cotton yarn, 42 tex cotton yarn, 34 tex viscose yarn and 34 tex 50:50/cotton: viscose blend yarn produced by the conventional rotor spinning unit are 13.80, 13.62, 7.99 and 9.86 cN/Tex respectively. However, corresponding to the yarns made using the modified rotor spinning unit, they are 15.59, 15.04, 8.67 and 10.61 cN/Tex respectively, increasing by a margin of 12.97 %, 10.38 %, 8.43 % and 7.59 %. Nevertheless, elongation of the modified rotor spun yarns does not show noticeable difference compared to that of conventionally spun yarns as shown in Figure 8.

**[Figure 7 here]**

**[Figure 8 here]**

In the ANOVA test, the $F$-value is compared to the critical value $F_{crit}$. If $F$-value ≥ $F_{crit}$, Sig. ($P$) Value ≤ $\alpha$ (here $\alpha = 0.05$), then it indicates that there is a significant difference between the group's variances. The ANOVA statistical results of tenacity and elongation of the spun yarns are presented in Figures 7 and 8, respectively. a-a means there is no significant difference between the two group's variances, while a-b means there is a significant difference between the two group's variances. Therefore, it can be seen from Figure 7 that the modified rotor spinning unit has a significant effect on the yarn tenacity. However, there is no statistically significant difference between means of the elongation of the spun yarns as seen from Figure 8. The ANOVA statistical results show that the modified rotor spinning system can improve the yarn tenacity.

*Unevenness*

The statistical analysis results of the yarn evenness and imperfections are also introduced in this paper, see Tables 3 to 6. A $P$-value smaller than the signification value indicates that the two means differ significantly at $\alpha = 0.05$. Therefore, it can be observed from Table 3 that there is a significant improvement in mass unevenness

(CV (%)) and the number of thin places (-50%), thick places (+50%) and neps (+280%) of the modified 34 tex cotton yarn. However, the results for 42 tex cotton yarn, 34 tex viscose yarn and 34 tex cotton/viscose blend yarn indicate that the effect of the modified design of the rotor spinning unit on CV (%), the number of thin places (-50%), thick places (+50%) and neps (+280%) is not significant.

**[Table 3 here]**

**[Table 4 here]**

**[Table 5 here]**

**[Table 6 here]**

*Hairiness*

Similarly, the comparison of average values of yarn hairiness (numbers of hairiness ≥ 3mm per meter) for each case studied, is introduced in Table 7. The average values of hairiness of the modified cotton yarns show a small difference with respect to that of the conventional rotor spun cotton yarns. The $P$-values for 34 tex and 42 tex cotton yarns are 0.250 and 0.091, respectively. This indicates that the hairiness between the modified and conventional rotor spun cotton yarns is not significantly different. However, both the viscose yarn and the blend yarn hairiness are reasonably lower than that of the conventionally spun yarns. The significance test results clarify that there is significant difference between means of hairiness of the viscose yarn and the blend yarn. This may be due to the different intrinsic properties between the viscose and cotton fibers.

**[Table 7 here]**

### *Fiber straightness*

The comparison of the fiber configuration in the rotor groove for the conventional and modified rotor spinning units is shown in Figure 9. It is to be noted that the percentage of fibers of Class 3 (trailing hooked) and Class 4 (leading hooked) for the modified rotor spinning unit are 5.20 % and 8.09 %, respectively. Compared with the 8.96 % and 15.67 % percentages obtained by the conventional rotor spinning unit, it concludes that the new unit generates a decrease of Class 3 and Class 4 fibers of respectively 41.96 % and 48.37 %. By using the modified rotor spinning unit, the amount of nearly straight fibers, Class 2 fibers, increases by 25.55 %. From Figure 9, the increase in the number of nearly straight fibers is mainly due to the decrease in the amount of trailing and leading hooked fibers. In other words, the new unit is very successful in generating straight fibers. However, the percentages of Class 6-8 (looped, folded and entangled fibers) have small differences between the two spinning conditions.

The improvement of fiber configuration is likely to be due to the following reasons. Firstly, the vortex inside the transfer channel inlet is decreased using the round transfer channel inlet corner and the bypass, which decreases the risk of fiber being trapped into the vortex and therefore reducing the number of straight fibers being bent. Secondly, the external air flowing from the bypass channel enters the transfer channel, increasing the air mass flow along the transfer channel. Also, the air velocity at the transfer channel inlet is more uniform in the modified condition, which is beneficial to fiber transportation. Thirdly, the air velocity in the fiber separation area is also increased, and this is also an effect from the bypass. This is helpful for fiber removal from the opening roller pins. Meanwhile, the increase of air velocity at the transfer channel inlet increases the possibility of fiber leading end being straightened and at the same time benefits the fiber transportation to the rotor. As the looped, folded and entangled fibers have a complex configuration (highly curly), the increase in air velocity along the transfer channel could hardly have effects on straightening these fibers. The number of these fibers (Class 6-8) remains almost the same.

Table 8 shows the analysis of variance of fiber orientation parameter *S*. The average value of *S* for the modified spinning unit condition is 0.1586, decreased by 32.77 % with respect to that for the conventional one. The signification value for the comparison of the means is 0.003, which indicates that fiber straightness is significantly improved by using the modified rotor spinning unit.

**[Figure 9 here]**

**[Table 8 here]**

## Conclusion

In this study, an extensive investigation to highlight the advantages on the yarn properties obtained when employing a new rotor spinning design was conducted. The conventional transfer channel was modified by rounding the transfer channel inlet corner and introducing a bypass channel as an air supply channel. The results from the simulations showed that the adverse vortex located at the transfer channel inlet and characteristic of conventional transfer channel units can be drastically reduced via using the new design. To evaluate the benefits of the new design in the yarn produced, a set of tests involving different raw materials for both conventional and the new unit were performed. Based on the results obtained experimentally, the following conclusions can be drawn:

The modification in the transfer channel will improve yarn tenacities significantly. Evenness and imperfections, i.e. CV (%), the number of thin places (-50 %), thick places (+50%) and neps (+280%), of the modified 34 tex cotton yarn showed significant improvements. Average hairiness of the modified cotton yarns showed a slight difference with respect to that of the conventionally spun cotton yarns.

However, hairiness of the modified viscose yarn and cotton/viscose blend yarn was significantly lower than that of the conventional yarn.

The fiber straightness test results reveal that the increase of yarn tenacity is mainly contributed by the decrease in the number of fibers with leading and trailing hooks. This also indicates that the airflow inside the transfer channel has an important effect on fiber configuration. Reducing air vortex and increasing air velocity in fiber transfer channel is helpful for fiber straightness and hence yarn properties.

## Funding

This work was supported by the Key Grant Project of Ministry of Education of the People's Republic of China (Grant 113027A).

## References

Erdumlu, N., Ozipek, B., Oztuna, A. S., & Cetinkaya, S. (2009). Investigation of Vortex Spun Yarn Properties in Comparison with Conventional Ring and Open-end Rotor Spun Yarns. *Textile Research Journal*, *79*, 585-595. Retrieved from http://journals.sagepub.com/doi/abs/10.1177/0040517508093590

Eldessouki, M., Ibrahim, S., & Farag, R. (2015). Dynamic properties of air-jet yarns compared to rotor spinning. *Textile Research Journal*, *85*, 1827-1837. Retrieved http://journals.sagepub.com/doi/abs/10.1177/0040517514563726.

Lord, P. R. (1971). The Structure of Open-End Spun Yarn. *Textile Research Journal*, *41*, 778-784. DOI: 10.1177/004051757504500502

Pillay, K. P. R., Viswanathan, N., & Parthasarathy, M. S. (1975). The Structure and Properties of Open-End Yarns: Part I: A Study of Fiber Configurations and Migration. *Textile Research Journal*, *45*, 366-372. DOI: 10.1177/004051757504500502

Koç, E., & Lawrence, C. A. (2006). Mechanisms of wrapper fibre formation in rotor spinning: An experimental approach. *Journal of the Textile Institute*, *97*, 483-492. DOI:10.1533/joti.2006.0199

Jin, Y., Cui, J., Li, X., & Chen, H. (2016). An investigation on the distribution of massive fiber granules in rotor spinning units. *Textile Research Journal*, *87*, 865-877. DOI: 10.1177/0040517516646054

Lin, H. T., Zeng, Y. C., & Wang, J. (2015). Computational simulation of air flow in the rotor spinning unit. *Textile Research Journal*, *86*, 115-126. DOI: 10.1177/0040517515586162

Chattopadhyay, R. (1988). Influence of the Yarn Formation Process on Fiber Configuration in Rotor Spun Yarn. *Textile Research Journal*, *58*, 674-676. Retrieved from https://doi.org/10.1177/004051758805801110

Murugan, R., Dasaradan, B. S., Karnan, P., & Senthilkannan, M. S. (2007). Fibre Rupture Phenomenon in Rotor Spinning. *Fibers and Polymers*, *8*, 665-668. Retrieved from https://doi.org/10.1007/BF02876006

Salhotra, K. R., & Chattopadhyay, R. (1982). Incidence and Mechanism of Fiber Breakage in Rotor Spinning. *Textile Research Journal*, *52*, 317-320. DOI: 10.1177/004051758205200503

Chattopadhyay, R., & Sarkar, S. (1986). Incidence of Fiber Reversal and Change in Fiber Configuration in Rotor Spinning. *Textile Research Journal*, *56*, 71-75. DOI: 10.1177/004051758605600112

Smith, A. C., & Roberts, J. W. W. (1994). Straightening of Crimped and Hooked Fibers in Converging Transport Ducts: Computational Modeling. *Textile Research Journal*, *64*, 335-344. DOI: 10.1177/004051759406400605

Lawrence, C. A., & Chen, K. Z. (1988). A Study of the Fibre-transfer-channel Design in Rotor-spinning. Part II: Optimization of the Transfer-channel Design. *Journal of the Textile Institute*, *79*, 393-408. DOI: 10.1080/00405008808658274

Lawrence, C. A., & Chen, K. Z. (1988). A Study of the Fibre-transfer-channel Design in Rotor-spinning. Part I: The Fibre Trajectory. *Journal of the Textile Institute*, *79*, 367-392. DOI: 10.1080/00405008808658273

Zhang, L. H., & Zhang, B. X. (1991). A Study of Fiber Transfer Channel in Rotor Spinning. *Journal of China Textile University*, *17*, 16-26. Retrieved from http://www.cqvip.com/QK/91942X/199106/661703.html

Kong, L. X., & Platfoot, R. A. (1996). Two-Dimensional Simulation of Air Flow in the Transfer Channel of Open-End Rotor Spinning Machines. *Textile Research Journal*, *66*, 641-650. DOI: 10.1177/004051759606601005

Kong, L. X., & Platfoot, R. A. (2000). Fibre transportation in confined channel with recirculations. *Computers and Structures*, *78*, 237-245. Retrieved from https://doi.org/10.1016/S0045-7949(00)00092-4

Kong, L. X., & Platfoot, R. A. (1997). Computational Two-Phase Air/Fiber Flow Within Transfer Channels of Rotor Spinning Machines. *Textile Research Journal*, *67*, 269-278. DOI: 10.1177/004051759706700406

Lin, H. T., Bergada, J. M., Zeng, Y. C., Akankwasa, N. T., Zhang, Y. Z., & Wang, J. (2018). Rotor spinning transfer channel design optimization via CFD. *Textile Research Journal*, *88*, 1244-1262. DOI: 10.1177/0040517517698985

Lawrence, C. A., & Jiang, R. K. (1996). A Study of the Mechanics of Fibre-straightening during Deposition in the Disc-spinning Process Part I: Theoretical Consideration. *Journal of the Textile Institute*, *87*, 23-36. DOI: 10.1080/00405009608659053

Lawrence, C. A. & Chiu, S. F. (1996). Part II: Comparison of Disc-Ring and Woolen Ring Spun Yarn Structure and Properties. *Textile Research Journal*, *66*, 164-172. Retrieved from https://doi.org/10.1177/004051759606600306

Lawrence, C. A. & Chen, K. Z. (1986). 16-High-Speed Photographic Studies of the Fibre Configuration during Transfer from the Opening Roller of a Rotor-Spinning Unit. *Journal of the Textile Institute*, *77*, 201-211. DOI: 10.1080/00405008608658410

Morton, W. E., & Summers, R. J. (1949). Fiber Arrangement in Card Slivers. *Journal of the Textile Institute Proceedings*, *40*, 106-116. DOI:

10.1080/19447014908664623

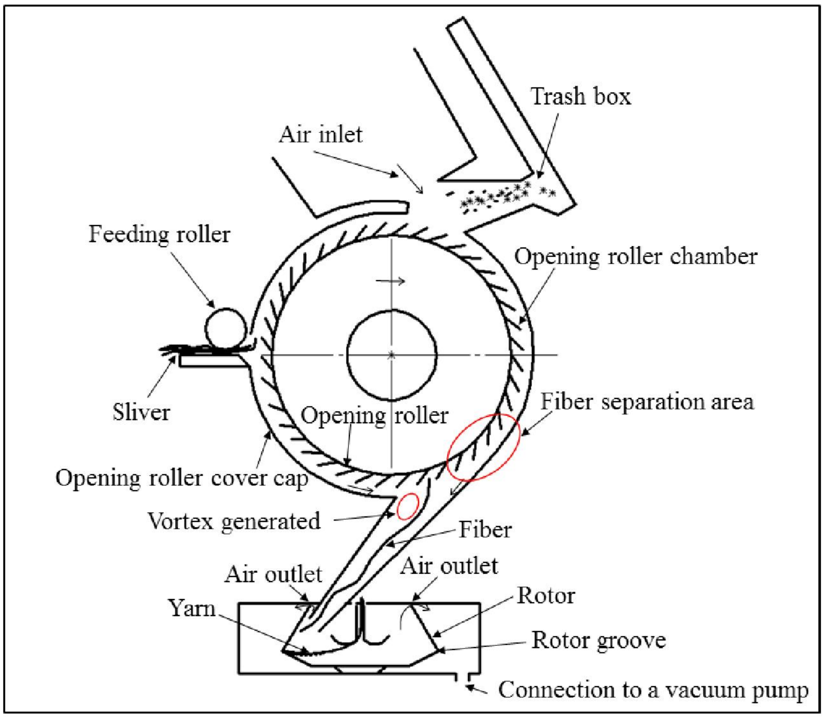


Figure 1. Schematic diagram of the conventional rotor spinning unit.

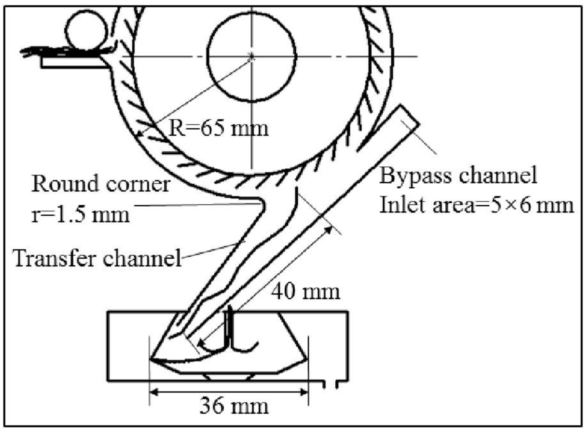


Figure 2. Schematic diagram of the modified rotor spinning unit.

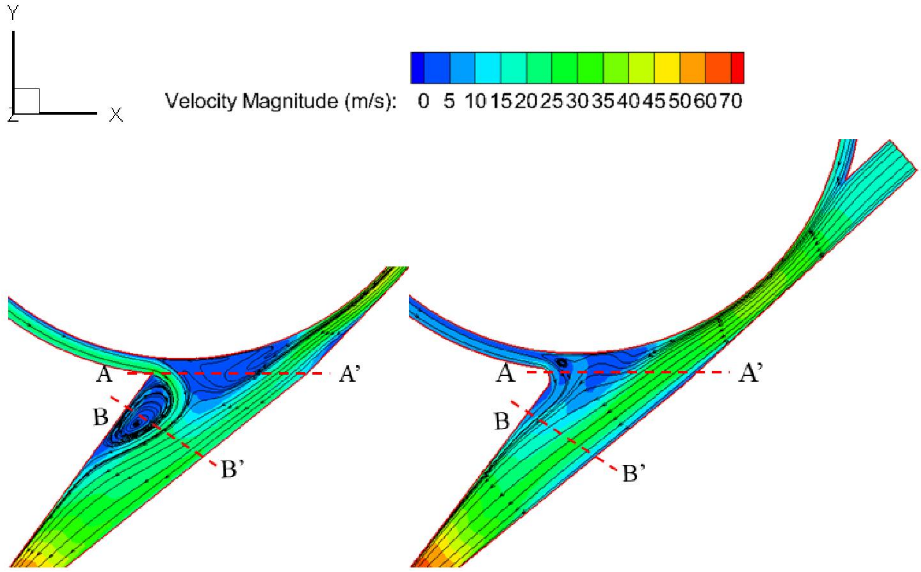


(a) conventional (b) modified

Figure 3. Streamlines of airflow in the transfer channel.

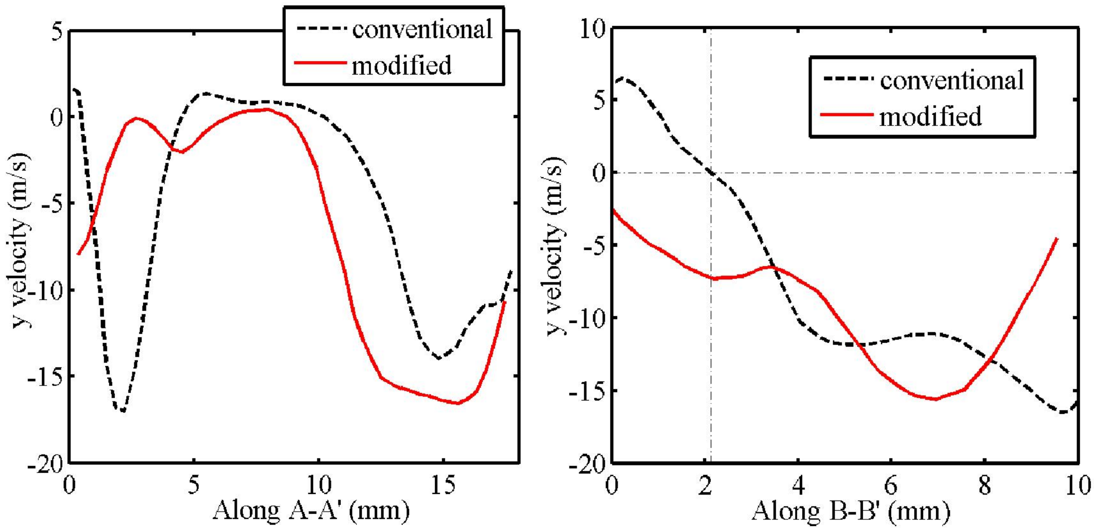


(a) A-A' (b) B-B'

Figure 4. Velocity distributions along A-A and B-B (see Figure 3).

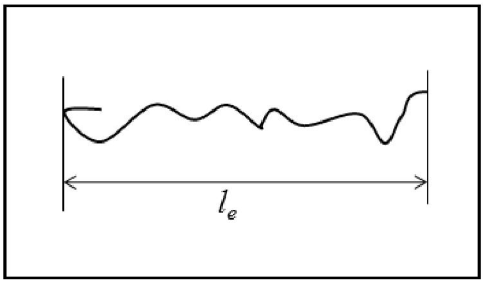


Figure 5. Image of fiber configuration in the rotor groove.

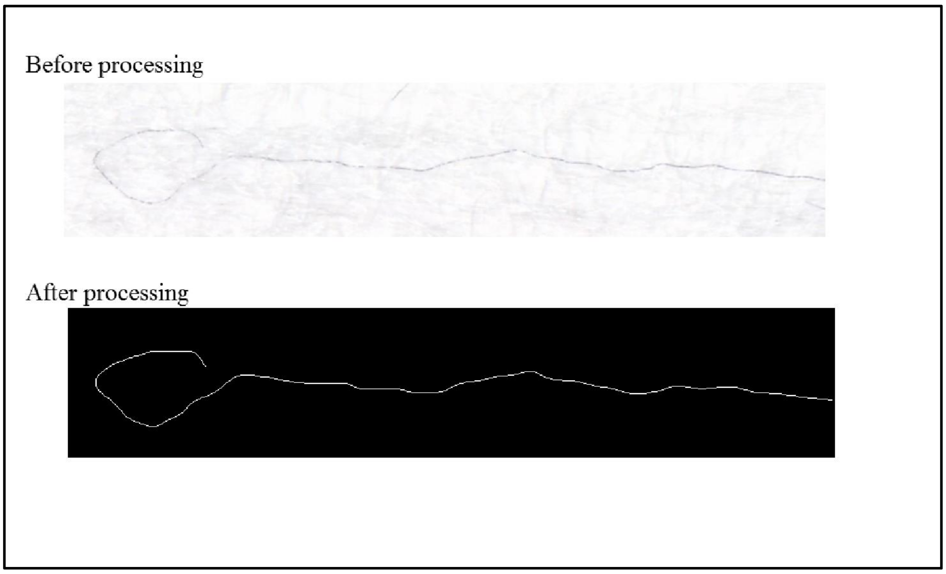


（a）Class 4 (leading hooked)

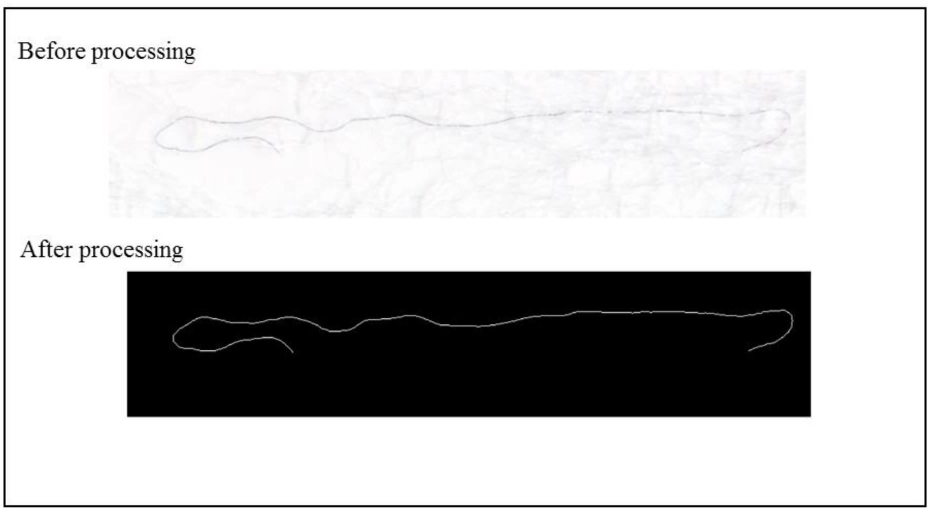


（b）Class 5 (both ends hooked)

Figure 6. Samples of fiber image obtained by scanning and after processing in MATLAB.

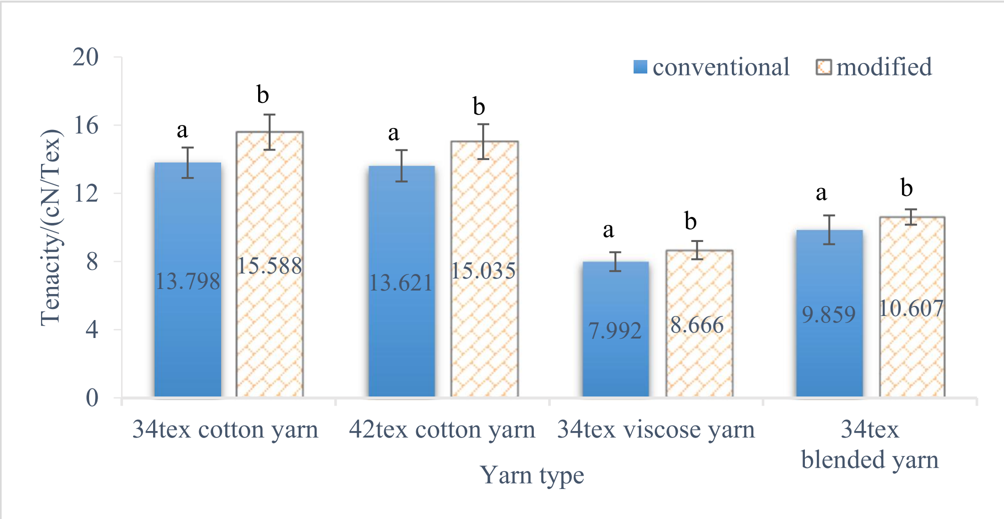


Figure 7. Average values of tenacities of yarn samples. a-b means there is a significant difference between the two group's variances, a-a means there is no significant difference between the two group's variances.

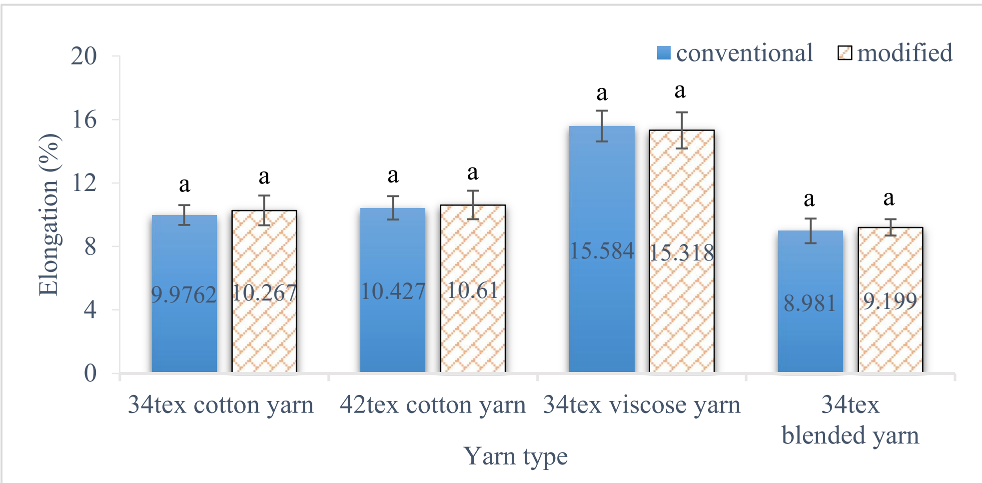


Figure 8. Average values of elongation of yarn samples. a-b means there is a significant difference between the two group's variances, a-a means there is no significant difference between the two group's variances.

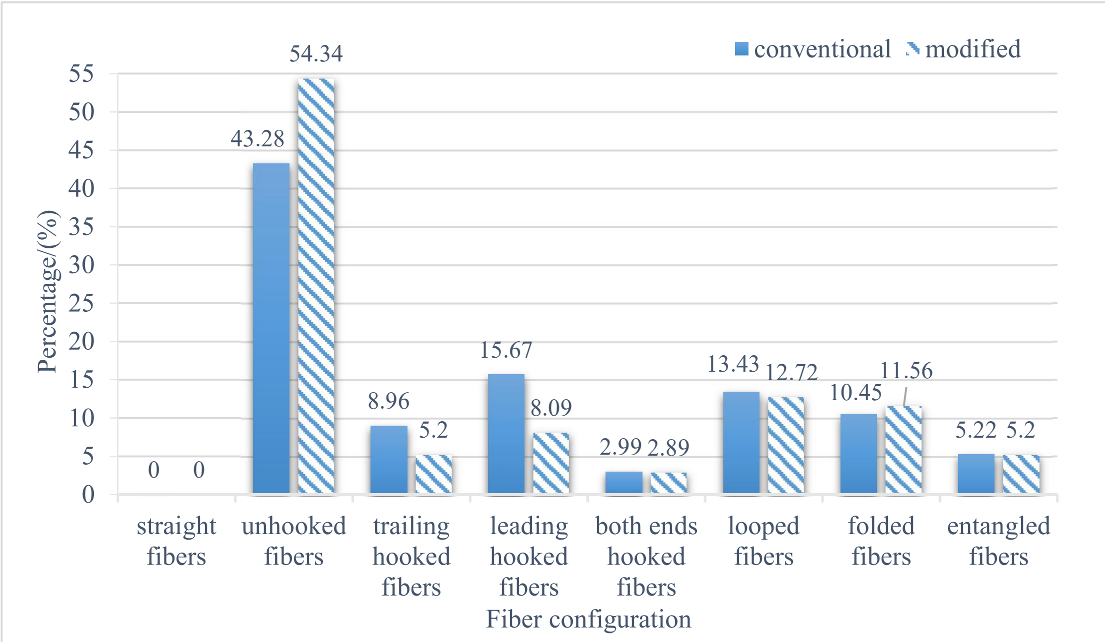


Figure 9. Comparison of the fiber configurations in conventional and modified spinning systems.

Table 1. Specifications of the raw materials and spinning conditions.

| Material | Cotton | Viscose | 50:50/Cotton: Viscose |
|---|---|---|---|
| Fiber length (mm) | 29 | 38 | |
| Fiber fineness (dtex) | 1.8 | 1.67 | |
| Sliver count (tex) | 4200 | 4312 | 3250 |
| Yarn count (tex) | 34, 42 | 34 | 34 |
| *Speeds of the rotor spinning unit, conventional and modified* | | | |
| Opening roller (rpm) | 6500 | 6500 | 6500 |
| Rotor (rpm) | 51000 | 51000 | 51000 |
| Yarn delivery (m/min) | 61.11, 68.75 | 60.44 | 60.44 |
| *Ambient conditions* | | | |
| T | 11±2℃ | | |
| R.H. | 50±2 % | | |

Table 2. Classification of fiber configuration in the rotor groove.

| Class No. | Description | Fiber shape |
|---|---|---|
| 1 | straight |  |
| 2 | unhooked (i.e., near straight) |  |
| 3 | trailing hooked |  |
| 4 | leading hooked |  |
| 5 | both ends hooked |  |
| 6 | looped |  |
| 7 | folded | 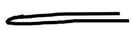 |
| 8 | entangled |  |
| Direction of fiber movement | | |

Table 3. Comparison of means of yarn evenness and imperfections of 34 tex cotton yarn (/km).

| Evenness and imperfections | Yarn type | *N* | Mean | *P*-Value | Evenness and imperfections | Yarn type | *N* | Mean | *P*-Value |
|---|---|---|---|---|---|---|---|---|---|
| | Co | 10 | 15.63 | | Thick places | Co | 10 | 92 | |
| CV (%) | Mo | 10 | 14.29 | 0.001 | (+50%) | Mo | 10 | 48 | 0.006 |
| Thin places | Co | 10 | 18 | | Neps | Co | 10 | 38 | |
| (-50%) | Mo | 10 | 2 | 0.016 | (+280%) | Mo | 10 | 6 | 0.002 |

Co: conventional rotor spinning unit; Mo: modified rotor spinning unit.

Table 4. Comparison of means of yarn evenness and imperfections of 42 tex cotton yarn (/km).

| Evenness and imperfections | Yarn type | *N* | Mean | *P*-Value | Evenness and imperfections | Yarn type | *N* | Mean | *P*-Value |
|---|---|---|---|---|---|---|---|---|---|
| | Co | 10 | 13.97 | | Thick places | Co | 10 | 32 | |
| CV (%) | Mo | 10 | 14.34 | 0.484 | (+50%) | Mo | 10 | 30 | 0.912 |
| Thin places | Co | 10 | 4 | | Neps | Co | 10 | 10 | |
| (-50%) | Mo | 10 | 20 | 0.274 | (+280%) | Mo | 10 | 2 | 0.455 |

Co: conventional rotor spinning unit; Mo: modified rotor spinning unit.

Table 5. Comparison of means of yarn evenness and imperfections of 34 tex viscose yarn (/km).

| Evenness and imperfections | Yarn type | *N* | Mean | *P*-Value | Evenness and imperfections | Yarn type | *N* | Mean | *P*-Value |
|---|---|---|---|---|---|---|---|---|---|
| | Co | 10 | 14.44 | | Thick places | Co | 10 | 22 | |
| CV (%) | Mo | 10 | 15.0 | 0.473 | (+50%) | Mo | 10 | 22 | 1.000 |
| Thin places | Co | 10 | 4 | 0.486 | Neps | Co | 10 | 28 | 0.880 |

| | | | | | | | |
|---|---|---|---|---|---|---|---|
| (-50%) | Mo | 10 | 8 | (+280%) | Mo | 10 | 30 |

Co: conventional rotor spinning unit; Mo: modified rotor spinning unit.

Table 6. Comparison of means of yarn evenness and imperfections of 34 tex blend yarn (/km).

| Evenness and imperfections | Yarn type | *N* | Mean | *P*-Value |
|---|---|---|---|---|
| | Co | 10 | 17.42 | |
| CV (%) | Mo | 10 | 17.18 | 0.613 |
| | Co | 10 | 36.7 | |
| Thin places (-50%) | Mo | 10 | 28.89 | 0.589 |
| | Co | 10 | 75.56 | |
| Thick places (+50%) | Mo | 10 | 72.2 | 0.819 |
| | Co | 10 | 16.67 | |
| Neps (+280%) | Mo | 10 | 6.67 | 0.116 |

Co: conventional rotor spinning unit; Mo: modified rotor spinning unit.

Table 7. Comparison of means of yarn hairiness (numbers of hairiness ≥ 3mm /m).

| Yarn type | | *N* | Mean | *P*-Value |
|---|---|---|---|---|
| | Conventional | 10 | 4.88 | |
| 34 tex cotton yarn | Modified | 10 | 5.64 | 0.250 |
| | Conventional | 10 | 11.0 | |
| 42 tex cotton yarn | Modified | 10 | 9.86 | 0.091 |
| | Conventional | 10 | 8.64 | |
| 34 tex viscose yarn | Modified | 10 | 4.54 | 0.000 |
| | Conventional | 10 | 11.62 | |
| 34 tex blend yarn | Modified | 10 | 4.94 | 0.000 |

Table 8. Analysis of variance of parameter *S*.

| Type | N | Mean | P-Value |
|---|---|---|---|
| Conventional | 100 | 0.2359 | 0.003 |
| Modified | 100 | 0.1586 | |